Soluble and supported carbonylation catalysts derived from rhodium–phosphonate–phosphane complexes

S. Bischoff [a,*], A. Weigt [a], H. Mießner [b], B. Lücke [a]

[a] *Institute for Applied Chemistry Berlin-Adlershof, Rudower Chaussee 5, 12489 Berlin, Germany*
[b] *Centre for Heterogeneous Catalysis (KAI e.V.), Rudower Chaussee 5, 12489 Berlin, Germany*

Abstract

Phosphonate–phosphanes form both chelate and open-chain complexes with rhodium, which can easily be converted into each other. This property has been used in the development of new and efficient carbonylation catalysts. During the catalytic cycle, the phosphane group is assumed to be coordinated to the transition metal, while the phosphoryl-oxygen of the phosphonate group is supposed to change between a free and a coordinated state, thus vacating or occupying a coordination site. IR studies support the hemilabile behaviour of surface Rh-complexes under the reaction conditions. Activation enthalpies, obtained for hemilabile rhodium catalysts in homogeneous methanol carbonylation, increased significantly with growing distance between phosphonate and phosphane group. Attempts of preparing stable rhodium complex catalysts adsorbed on silica or alumina for slurry-phase or vapour-phase carbonylations failed. Activated carbon has been shown to be a suitable support for hemilabile rhodium complexes, but normal diffusion of reactants begins to limit the carbonylation rate over the supported catalysts.

Keywords: Phosphonate–phosphanes; Hemilabile catalysts; Rhodium; Methanol; Carbonylation; Phosphane complexes; Supported catalysts

1. Introduction

Mixed bidentate phosphane ligands such as ether–phosphanes [1–3], phosphane oxide–phosphanes [4], phosphanpyridines and 10-phosphano-amines [5] containing O- or N-donor groups and a strongly electron-donating phosphane group, are known to enhance activities or selectivities of Rh-catalysed carbonylations. Also other transition metals form hemilabile O,P–chelate complexes, which have been extensively reviewed by Lindner [6]. It has been suggested that the oxygen-donating site of the bidentate ligand changes between a coordinated and an uncoordinated state during the catalytic cycle, thus forming chelate and open-chain metal complex structures [1,4]. The intramolecular generation and occupance of free coordination sites is assumed to accelerate rate-determining steps in the methanol carbonylation route. Heterobidentate complexes catalysed not only carbonylations effectively but also hydrogenation [7], hydrosilylation [8], and ethylene polymerization [9]. The phosphane sulphide–phosphane, $Ph_2PCH_2P(S)Ph_2$, was reported to form a catalyst that is eight times more active in methanol carbonylation than the conventional Monsanto-catalyst [10]. It should be noted that no evidence for hemilabile behaviour was found for the new catalyst.
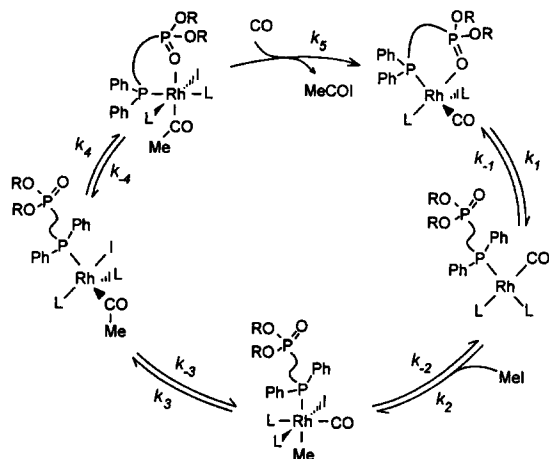
* Corresponding author.

Fig. 1. Methanol carbonylation with hemilabile Rh complex catalysts.

Rhodium complexes with phosphonate–phosphanes [11] appeared as promising catalyst precursors because they form hemilabile complexes, which should enhance the necessary formation of free coordination sites in Rh^I-intermediates by ring-opening of chelate structures and facilitate the generation of the more oxophilic Rh^{III}-intermediates by O,P–chelate formation (Fig. 1). The concept of hemilabile catalysts with chelate structures involved in rate-determining steps implies that the distance and structure between the phosphane and the phosphonate group should affect the carbonylation activity. To examine this hypothesis, we studied the activity of new rhodium complex catalysts
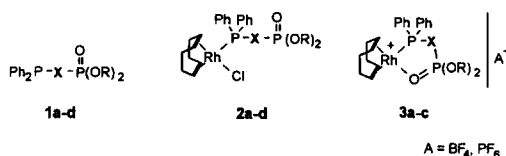
	X	R
a	- CH₂-	^{i}Pr
b	- CH₂CH₂-	Me, Et
c	- CH₂CH₂CH₂-	^{i}Pr
d	-⟨O⟩-	^{i}Pr

Fig. 2. Ligands and rhodium–phosphonate–phosphane complexes.

derived from ligands **1a–d** (Fig. 2) in homogeneous methanol carbonylation.

The phosphonate group was furthermore expected to facilitate surface-anchoring of the transition metal complexes on oxidic materials such as silica or alumina. We prepared several supported catalysts with rhodium complexes using alumina, silica and activated carbon as carrier materials and will report on their properties in slurry- and vapour-phase carbonylation.

2. Experimental

2.1. Materials

Methanol, methyl iodide and methyl acetate (Merck) were used as received. Tetrahydrofuran was distilled from sodium/benzophenone. Dichloromethane was dried over molecular sieve, type 3A (Alfa Products). Activated carbon (Desorex ED 47, Lurgi, specific surface area 800 m²/g), alumina (Aluperl 1039/6, GS 2363, Kalichemie, specific surface area 52 m²/g, and silica (large-pore silica, Alfa Products, specific surface area 270 m²/g) were dried at 250°C in vacuum (< 30 Pa) for 4 h and stored in a desiccator. Particle size fractions between 0.3 and 0.8 mm were used for the preparation of support catalysts. The preparation and characterisation of the heterobidentate rhodium complexes are described elsewhere [11,12]. Stirring of an aqueous solution of NaOH with a solution of **1b** in CH₂Cl₂ at 40°C afforded the corresponding half-ester, which was neutralized by HCl. After evaporation of CH₂Cl₂, the half-ester was dissolved in deoxygenated tetrahydrofuran and refluxed over Al₂O₃ or SiO₂ for 24 h. Unreacted half-ester was removed from the support by extraction with tetrahydrofuran in a Soxhlet apparatus. [ClRh(cod)]₂ was dissolved in CH₂Cl₂ and allowed to react with the phosphane-modified oxides at room temperature for 24 h. Supported catalysts for vapour-phase carbonylations were prepared by impregnation of activated carbon,

silica and alumina with **2a, 2b**, [ClRh(cod)]$_2$, [ClRh(CO)(dppe)] (dppe: Ph$_2$P–(CH$_2$)$_2$–PPh$_2$), [ClRh(cod)(dppe–O)] [4] (dppe–O: Ph$_2$P–(CH$_2$)$_2$–P(O)Ph$_2$) and [(dppp)Rh(CO)Cl]$_2$ [13] (dppp: Ph$_2$P–(CH$_2$)$_3$–PPh$_2$) dissolved in CH$_2$Cl$_2$. Total metal loading varied between 0.1 and 0.5 wt.%.

2.2. Catalytic runs

Catalytic activities of the soluble Rh-catalysts were tested in a stirred 100-ml autoclave made of stainless steel. To exclude air, the autoclave was filled with 100 mmol methanol using Schlenk techniques, 6–48 mmol methyl iodide, 0.05–0.2 mmol rhodium complex, and methyl acetate was added to reach a total volume of 25 ml. After pressurizing with CO (1.5 MPa cold), the filled autoclave was heated to a reaction temperature between 120 and 195°C and then the pressure was adjusted to 3 MPa. During the catalytic runs, the reaction pressure was kept constant at this value with a pressure regulator. The carbonylation rate was monitored by recording the rate of CO uptake from a reservoir. Carbonylation activity was calculated from the initial CO conversion rate (CO conversion < 20%).

Slurry-phase carbonylations were carried out in a 250-ml autoclave equipped with a fixed catalyst basket and a magnetic stirrer, using 19 to 50 g of supported catalysts. The autoclave was filled to a volume of 122 ml with a mixture of methanol (8.21 mol/l), methyl iodide (1.02 mol/l) and acetone (8.2 mol/l, internal standard for GC) and the reaction was conducted at 180°C and 5 MPa. The conversion was followed by GC analysis of 10 to 20 samples taken at certain time intervals. After the catalytic runs, the solid catalysts were washed with acetone and used again. The Rh contents of the catalysts and the filtered solutions were determined by atom absorption spectroscopy.

A continuous flow type reaction apparatus with a fixed bed was used for the vapour-phase carbonylations. The catalysts (400–600 mg) were investigated without any activation procedure. The reactor (made of a stainless steel tube, inner diameter 6 mm) was heated to reaction temperature in an Ar-stream under atmospheric pressure. CO was fed to build up the reaction pressure between 0.5 and 2 MPa. The mixture
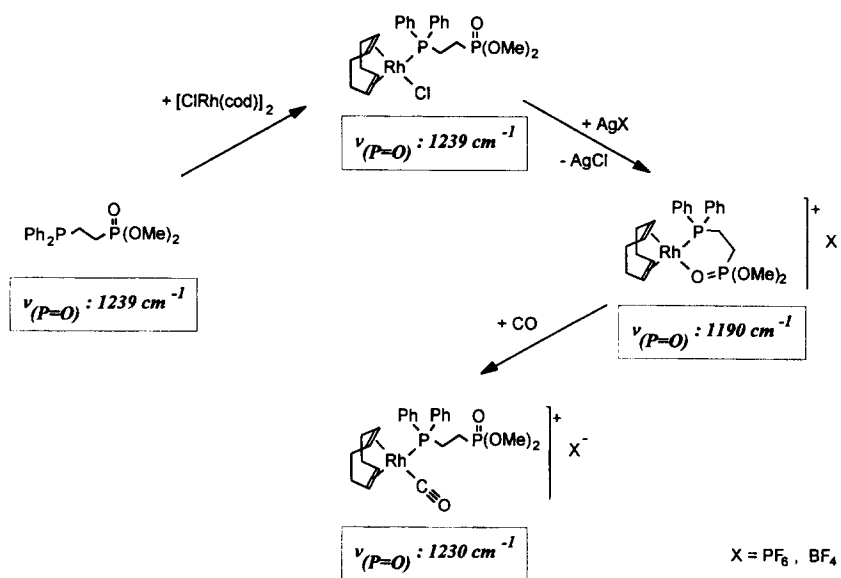

Fig. 3. Reactions and IR data of complexes derived from **1b** [12].

of methanol and the promoter methyl iodide was introduced with a Shimadzu LC 10AD HPLC pump. Product gas analysis was conducted with on-line GC. Yields of the products and selectivities of the reaction were calculated based on the substrate consumed.

In-situ IR investigations were carried out with 20–50 mg of self-supporting catalyst tablets in a quartz cell. The transmission spectra were recorded with a BIORAD FTS 60A-FTIR spectrometer. For comparison, spectra were related to those of pure silica or — in the case of CO-adsorption — to the starting spectrum. For interpretation, spectra of the pure substances [ClRh(cod)$_2$], **1b**, **2b**, dppe, [ClRh(CO)(dppe)] in KBr were employed, and literature data for model complexes [14] considered.

3. Results and discussion

3.1. The hemilabile character of phosphonate–phosphane–Rh complexes

Both, cyclic and open-chain complexes were isolated after stoichiometric reactions at mild conditions [12]. The catalyst precursors **2a–c** were smoothly converted with AgBF$_4$ or AgPF$_6$ into the halogen-free chelate complexes at room temperature and the ring-opening was easily achieved with CO at room temperature and atmospheric pressure. Fig. 3 illustrates this for complexes derived from **1b**. Reversibility of the ring-opening under reaction-like conditions is assumed from IR investigations of supported complexes (see below). IR shifts in the stretching band of the phosphoryl group $\nu_{(P=O)}$ to lower values in **3a–c** (KBr-pellet or solution) indicate the coordination of phosphoryl oxygen.

^{31}P NMR data are listed in Table 1. The signals of the coordinated phosphane groups are shifted towards lower fields with respect to the free ligands. The coupling constants J_{PRh} indicate square–planar structures of open-chain and chelate complexes. The chelate structures of **3a–c** are confirmed by low field shifts of the

Table 1
^{31}P-NMR data of ligands and Rh complexes [12]

	$\delta_{P=O}$	J_{PORh}	J_{PP}	$\delta_{Phosphane}$	J_{PRh}
Ligands					
1a	24.91 (d)	–	45.9	– 25.32 (d)	–
1b	34.50 (d)	–	62.0	– 12.10 (d)	–
1c	29.71 (d)	–	2.9	– 17.37 (d)	–
1d	16.13	–	–	– 5.19	–
Open-chain complexes					
2a	21.33 (d)	–	16.9	21.51 (dd)	156.8
2b	32.80 (d)	–	63.0	26.80 (dd)	150.0
2c	29.28 (d)	–	4.9	26.60 (dd)	151.6
2d	15.17	–	–	30.87 (d)	150.8
Chelate complexes					
3a	48.85 (dd)	5.7	50.8	14.69 (dd)	149.6
3b	38.79 (dd)	2.9	13.1	21.21 (dd)	154.0
3c	40.13 (d)	8.1	–	23.74 (dd)	153.5

Measured in CHCl$_3$ with external standard (85% H$_3$PO$_4$), δ in ppm, J in Hz, d = doublet, dd = double-doublet.

phosphoryl–phosphorus signal ($\delta_{P=O}$), compared to **1a–c**, **2a–c** and additionally by its coupling with rhodium (J_{PORh}). Considering the IR spectra of **3a–c**, it is concluded that the P=O-groups and not the P–O–R′-groups act as oxygen donors.

3.2. Homogeneous rhodium–phosphonate–phosphane catalysts

The methanol carbonylation to acetic acid can roughly be formulated as a sequence of oxidative addition of the promoter methyl iodide, followed by methyl group migration to a CO ligand and reductive elimination of acetyl
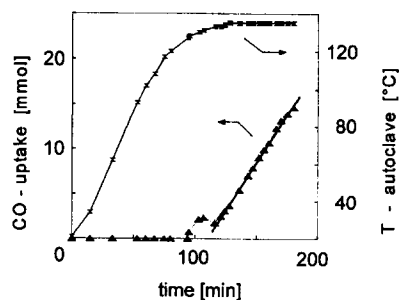

Fig. 4. Typical autoclave experiment with soluble catalysts.

Table 2
Ligand effects on activation parameters in homogeneous Rh-catalysed methanol carbonylation

	Rh/AC [a]	None [b]	PPh$_3$ [c]	dppe [d]	2a	2b	2c	2d
ΔH^* [kJ/mol]	20.4	67.5	54.9	27.5	38.6	55.2	61.8	76.0
$\pm$	9.2	13.1	5.4	6.2	3.4	5.2	5.3	9.1
ΔS^* [J/mol/K]	−233	−112	−141	−211	−179	−141	−126	−90
$\pm$	22	32	13	15	8	12	12	22

[a] Slurry-phase, [ClRh(cod)]$_2$/activated carbon, rough estimation.
[b] [ClRh(cod)]$_2$.
[c] [ClRh(cod)]$_2$ + 2 PPh$_3$.
[d] [ClRh(CO)(dppe)].

iodide induced by CO attack. The promoter is regenerated from methanol and HI, the last being liberated in the fast and irreversible protolysis of acetyl iodide.

A typical kinetic run is described in Fig. 4. The linearity of the plot for the CO uptake vs. time shows the zero-order of the substrate methanol. Second-order rate constants k_i (l mol^{-1} s^{-1}) were related to the concentrations of rhodium and methyl iodide, and determined in a temperature range between 120 and 195°C. The rate constants obtained for various Rh-catalysts were used for the calculation of activation parameters. Activation enthalpies and entropies resulting from 6 to 8 rate constants per catalyst are summarised in Table 2. The activation enthalpies change significantly over a wide range. It is interesting that activation enthalpies obtained for the hemilabile catalyst precursors 2a–d increased with growing distances between

the phosphonate- and phosphane-group. The highest activation enthalpy was found for the p-phenylene-bridged phosphonate–phosphane ligand 1d, which can not form chelate complexes. This indicates that chelate structures are involved in one of the rate-limiting steps. Oxidative addition of methyl iodide does not seem to be the only rate-determining step, as it is suggested by the decrease of its reaction order to values about 0.5 in the presence of hemilabile ligands. It is known, that phosphane ligands can stabilize acyl species and thus slow down reductive elimination [15]. Rate-limiting steps other than oxidative addition of methyl iodide can be the reductive elimination of acetyl iodide (Fig. 1: $k_4 \cdot k_5$) or the methyl group migration (Fig. 1: k_3). None of these alternatives can clearly be appointed as being more likely with the given kinetic data.
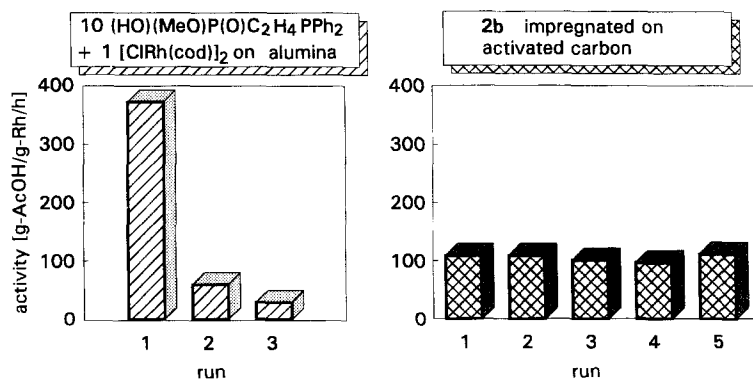
The apparently low activation enthalpy esti-

Fig. 5. Activity of supported hemilabile complexes after repeated use in slurry-phase methanol carbonylation.

mated (only from three rate constants) for Rh supported on activated carbon is probably caused by diffusion control. Observations in the vapour-phase methanol carbonylation (see below) confirmed this assumption.

However, a general superiority of the hemilabile catalysts compared to known systems can not be postulated with the results in Table 2. At certain temperatures the hemilabile catalysts appear to be superior, but the opposite can be observed at another temperature, which may well illustrate that the comparison of activities at a more or less arbitrary chosen temperature is sometimes questionable.

The hemilabile complex precursors **2a–d** led to generally higher activation entropies than the bisphosphane complex precursor [ClRh(CO)(dppe)]. This can be explained with the generation of open-chain structures of the phosphonate–phosphane complexes during the oxidative addition step, creating additional degrees of freedom for bond-rotation and vibrations.

3.3. Slurry-phase methanol carbonylation

Fig. 5 compares the activities of hemilabile complexes supported on alumina or activated carbon after repeated use. The rapid activity decline of the alumina supported catalyst, prepared by reaction of the half-ester of **1b** with surface hydroxyl groups, is caused by Rh losses (> 90% after the third run) into the liquid-phase. Catalysts prepared by impregnation of **2b** on alumina showed the same behaviour. The observed stability of the catalyst supported on activated carbon is only an apparent one — the Rh loss was significant also at this system (42% after the fifth run), but it seems that diffusion control of the carbonylation rate, which is in good agreement with the lower initial activity of the carbon supported catalyst, concealed the leaching effect. Also other attempts to prepare stable slurry-phase catalysts for methanol carbonylation on the base of phosphonate–phosphanes failed.
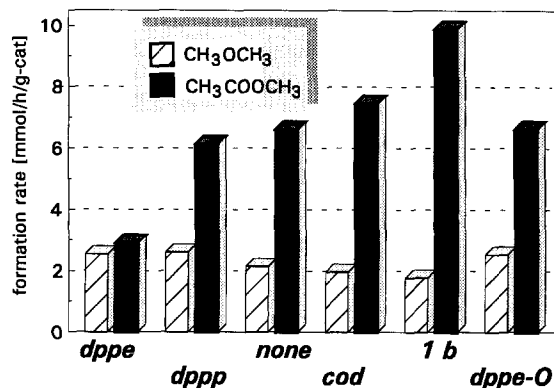

Fig. 6. Ligand effects on the activity of Rh complexes supported on activated carbon. 0.5 mol.% Rh, 180°C, 2 MPa, W/F = 2 g cat. h/mol, CO/MeOH/MeI = 100/19/1. dppe: $Ph_2PCH_2CH_2PPh_2$, dppp: $Ph_2PCH_2CH_2CH_2PPh_2$, dppe-O: $Ph_2PCH_2CH_2P(O)Ph_2$, cod: 1,5-cyclooctadiene.

3.4. Supported rhodium–phosphonate–phosphane catalysts

Phosphonate–phosphanes enhanced also activities in vapour-phase methanol carbonylation (Figs. 6 and 7). The phosphane oxide–phosphane dppe–O, which is known to enhance the homogeneous carbonylation [4], did not improve the activity of the carbon-supported catalyst. Strongly coordinated chelate ligands like dppe can even suppress the activity, possibly by blocking coordination sites necessary for the
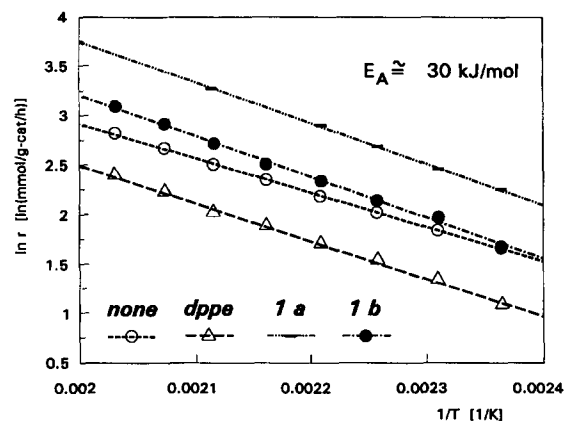

Fig. 7. Ligand effects on activation parameters of activated carbon-supported Rh catalysts, 0.5 wt.% Rh, 2 MPa, 4 g cat. h/mol, CO/MeOH/MeI = 100/19/1.
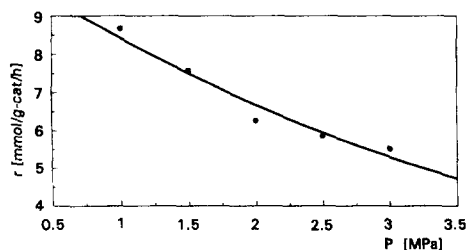
Fig. 8. Carbonylation activity of Rh on activated carbon vs. total pressure.Ar/CO/MeOH/Mel = X/50/90/1, T = 180°C. X = 0, 35, 70, 105 and 140 corresponding to 1, 1.5, 2, 2.5 and 3 MPa reaction pressure. W/F reactants = 2 g cat. h/mol.

Fig. 10. FTIR spectra of silica-supported 2b after various treatments.

carbonylation. In contrast to the results obtained for the homogeneous reaction, no significant ligand effects on the activation energies were observed, when the methanol carbonylation was conducted in the vapour-phase using activated carbon supported complexes (Fig. 7). Normal diffusion of reactants, as indicated by the influence of the total pressure on the activity (Fig. 8), begins to limit the activity of the supported Rh-complexes and leads to the observed uniform activation energies of about 30 kJ/mol.

While no indication for surface or vapour-phase migration of hemilabile ligands or Rh was found for activated carbon supported catalysts, the catalysts prepared by impregnation of alumina and silica with 2b, [ClRh(cod)]$_2$ and [ClRh(CO)(dppe)] deactivated after several
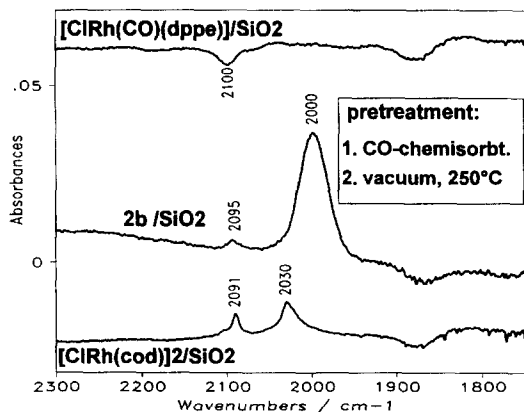
hours under vapour-phase carbonylation conditions. However, silica was a useful support for IR investigations. FTIR spectra of supported Rh-complex precursors revealed that the bisphosphane ligand dppe hinders the formation of stable carbonyls. This is in accordance with the lower carbonylation activity of the supported dppe-complex (Fig. 6). The observed formation of $Rh^I(CO)_2^+$ dicarbonyl species in the presence of CO shows that two coordination sites can easily be substituted in the case of supported [ClRh(cod)]$_2$ and 2b, while the ligand dppe is significantly harder to substitute. Under decarbonylation conditions, the hemilabile ligand 1b stabilizes mono-carbonyl species, possibly by using its second ligand function (Fig. 9). These species have a remarkable thermal stability (250°C), and can be converted again into dicarbonyl species with increasing CO partial pressure even at elevated temperatures (Fig. 10).

4. Summary

New hemilabile Rh-catalysts for carbonylations have been developed on the base of phosphonate–phosphanes and their efficiency was shown in methanol carbonylation. Structures with both monodentate and chelating coordination of the phosphonate–phosphane ligands were

Fig. 9. FTIR spectra of Rh complexes on silica after CO exposure and subsequent evacuation at 250°C.

obtained during the catalyst preparation. Activation parameters determined for various homogeneous hemilabile catalysts indicate the importance of both structures in the catalytic cycle. IR data of a supported Rh–phosphonate–phosphane complex suggest that the weakly coordinating phosphonate group allows the formation of free coordination sites. Although the above results are in accordance with hemilabile behaviour of the Rh–phosphonate–phosphane catalysts, no direct evidence has been presented in this study. The new hemilabile complexes afford also stable catalysts when they are supported on activated carbon, but diffusion of reactants at higher pressures begins to limit the intrinsic high activity of the supported complexes.

Acknowledgements

References

[1] E. Lindner, H.A. Mayer and P. Wegner, Chem. Ber., 119 (1986) 2616.
[2] E. Lindner, A. Sickinger and P. Wegener, J. Organomet. Chem., 349 (1988) 75.
[3] E. Lindner, A. Bader, H. Bräunling and R. Jira, J. Mol. Catal., 57 (1990) 291.
[4] R.W. Wegmann, A.G. Abatjoglou and A.M. Harrison, J. Chem. Soc., Chem. Commun., (1987) 1891; R.W. Wegmann and A.G. Abatjoglou, PCT Int. Appl. WO 8600888 (1986), C.A., 105 (1987) 174788.
[5] C. Abu-Gnim and I. Amer, J. Mol. Catal., 85 (1993) L275; C. Abu Gnim and I. Amer, J. Chem. Soc., Chem. Commun., (1994) 115.
[6] A. Bader and E. Lindner, Coord. Chem. Rev., 108 (1991) 27.
[7] W.S. Knowles, Acc. Chem. Res., 16 (1983) 106.
[8] Z.M. Michalska, J. Mol. Catal., 19 (1983) 345.
[9] K.O. Starzewski and J. Witte, Angew. Chem. Int. Ed. Engl., 24 (1985) 599.
[10] M.J. Baker, M.F. Giles, A.G. Orpen, M.J. Taylor and R.J. Watt, J. Chem. Soc., Chem. Commun., (1995) 197.
[11] J. Freiberg, A. Weigt and H. Dilcher, J. Prakt. Chem., 335 (1993) 337.
[12] A. Weigt and S. Bischoff, Phosphorus, Sulphur, Silicone, 102 (1995) 91.
[13] A.R. Sanger, J. Chem. Soc., Dalton Trans., (1977) 120.
[14] A. Vizi-Orosz, G. Pályi and L. Markó, J. Organomet. Chem., 57 (1973) 379; A. Theolier, A.K. Smith, M. Leconte, J.M. Basset, G. Zanderighi, R. Psaro and R. Ugo, J. Organomet. Chem., 191 (1980) 415; A. Vizi-Orosz, R. Ugo, R. Psaro, A. Sironi, M. Moret, C. Zucchi, F. Ghelfi and G. Pályi, Inorg. Chem., 33 (1994) 4600.
[15] K.G. Moloy and R.W. Wegmann, Organometallics, 8 (1989) 2883.